Effect of Zinc, Copper, and Calcium on the Structure and Stability of Serum Amyloid A†

Limin Wang and Wilfredo Colón*

Department of Chemistry and Chemical Biology, Rensselaer Polytechnic Institute, 110 8th Street, Troy, New York 12180

Received December 21, 2006; Revised Manuscript Received February 26, 2007

ABSTRACT: Serum amyloid A (SAA) is a highly conserved acute phase reactant protein, and its concentration in serum can increase up to ∼1000 times after an inflammatory stimuli. SAA is mainly associated with high-density lipoproteins in serum, and its main function appears to involve cholesterol transport and lipid metabolism. However, SAA has also been associated with many other functions and a number of diseases, although these potential links remain poorly understood. The three-dimensional structure of SAA is not known, but we have shown that murine SAA2.2 can exist in solution as a marginally stable hexamer, which at 37 °C dissociates to a monomeric species that misfolds irreversibly and self-assembles into amyloid fibrils. Thus, the structure and function of SAA in vivo appear to be modulated when it binds to other proteins or small ligands. Herein, the effect of copper (Cu^{2+}), zinc (Zn^{2+}), and calcium (Ca^{2+}) on the structure and stability of SAA2.2 in aqueous solution was examined using various probes of quaternary, tertiary, and secondary structure. At different concentrations of metals, including those found in the serum, the results show that the structure and stability of SAA2.2 are differently affected depending on the metal type and concentration. Copper (10−100 μM) was found to shift the equilibrium from hexamer to monomer without affecting significantly the stability of the tertiary and secondary structure of SAA2.2. In contrast, zinc (1−10 μM) bound to SAA2.2 and stabilized its quaternary, tertiary, and secondary structure. Calcium (1−10 mM) destabilized all elements of SAA2.2 structure and induced its aggregation at 10 mM. Complete aggregation of SAA2.2 was also observed when it was incubated with 1 mM Cu^{2+} or Zn^{2+}, further demonstrating the tenuous structure and stability of SAA2.2. Thus, these results suggest that the many functional and pathological roles attributed to SAA may rely on its precarious structure, modulated by its interaction with ligands under homeostasis conditions and during the acute phase response.

Serum amyloid A (SAA)[1] is one of the main acute phase proteins expressed by the liver and is predominantly found in plasma bound to the third fraction of high-density lipoprotein (*1*, *2*). SAA has been found in many vertebrate species, and comparison of the different SAA genes demonstrates that it is a highly conserved protein (*3*). Inflammatory stimuli like tissue injury, trauma, and infection can dramatically enhance its hepatic expression, resulting in a serum concentration of ∼1 mg/mL (*4*, *5*). SAA is also constitutively expressed in many tissues and cells (*6*−*9*), and its concentration has been found to increase in various cells (*10*−*14*). The tremendous expression levels of a highly conserved protein suggest that SAA may have host-protective roles during an inflammatory response; however, these presumed immune functions remain unknown. In light of the recognized role of inflammation in the pathology of many diseases (*15*−*18*), including atherosclerosis, cancer, and Alzheimer's disease, it is interesting that SAA has also been linked to the pathology of these and other diseases (*6*, *19*−*22*). Although the relationship between SAA and disease remains poorly understood, perhaps the persistently high concentration of SAA in plasma or in specific tissues during inflammation may have pathological consequences. One particularly well-known case is the disease amyloid A (AA) amyloidosis, also known as reactive or secondary amyloidosis, which is characterized by the deposition of SAA fibrils in various organs. AA amyloidosis was originally observed as a secondary and usually fatal effect in patients with chronic inflammatory diseases, such as rheumatoid arthritis and tuberculosis, and remains one of the most common systemic amyloid diseases worldwide (*23*, *24*). The amyloid deposits in AA amyloidosis are usually composed of the 76 N-terminal residues of SAA, although longer fragments, including the full-length protein, are also present (*25*−*27*).

Despite its small size (∼12 kDa) and the four decades since SAA was linked to AA amyloidosis, its three-dimensional structure remains undetermined due to the low solubility of the HDL-free protein. We previously reported that mouse isoform SAA2.2, which is resistant to amyloid

† This work was supported by grants from the American Heart Association and the National Institutes of Health (R01NS042915) to W.C.

* To whom correspondence should be addressed: Department of Chemistry and Chemical Biology, Rensselaer Polytechnic Institute, 110 8th Street, Troy, NY 12180. E-mail: colonw@rpi.edu. Telephone: (518) 276-2515. Fax: (518) 276-4887.

[1] Abbreviations: SAA, serum amyloid A; CD, circular dichroism; H_6:M_1, SAA2.2 hexamer to monomer ratio; λ_{max}, emission wavelength of maximum fluorescence; MOPS, 3-(*N*-morpholino)propanesulfonic acid; MRE or [θ], molar residue ellipticity; T_m, transition midpoint temperature; UV, ultraviolet.

10.1021/bi602629y CCC: $37.00
Published on Web 04/11/2007

formation in vivo, forms a hexamer in solution with a putative central pore (*28*). The SAA2.2 hexamer is marginally stable, losing most of its structure at 37 °C or in 2 M urea, suggesting that SAA2.2 may be a natively unfolded protein in vivo (*29*, *30*). Interestingly, the monomeric but not hexameric SAA2.2 was found to bind HDL particles in vitro, raising further questions about the physiological relevance of hexameric SAA2.2 or how it may be stabilized in vivo (*31*). The large number of diverse functions that have been linked to SAA and its dual constitutive and acute phase roles suggest that SAA may exist in different oligomeric or conformational forms that may be modulated by the concentration of SAA and/or its binding to ligands, including lipids, heparin, other proteins, and metal ions.

In this study, we focused on probing the interaction of hexameric SAA2.2 with zinc (Zn^{2+}), copper (Cu^{2+}), and calcium (Ca^{2+}) for several reasons. First, during inflammation, there are changes in Zn^{2+} metabolism and its serum concentration decreases (*32*, *33*), which is particularly noteworthy since this metal is known to play an important although poorly understood role in the immune system (*34*−*37*). Second, the concentration of Cu^{2+} increases during inflammation (*38*, *39*). It has also been shown that dietary copper deficiency may be associated with hypercholesterolemia and abnormal lipoprotein metabolism (*40*), conditions that overlap with the main presumed function of SAA (i.e., cholesterol metabolism) (*41*, *42*). Third, there is a putative Ca^{2+} binding site (GPGG) in SAA (*43*), and amyloid A deposits have been found to be rich in Ca^{2+} (*44*). Also, serum amyloid P, a common component found in all types of amyloid deposits in vivo, can bind to amyloid fibrils in a Ca^{2+}-dependent manner (*45*). Furthermore, numerous studies have found that bivalent cations such as Cu^{2+}, Zn^{2+}, and Ca^{2+} have a significant effect on the amyloidogenicity of various proteins, including PrP in prion disease (*46*, *47*), A-β in Alzheimer's disease (*48*−*53*), α-synuclein in Parkinson's disease (*54*−*56*), and β-2-microglobulin in renal dialysis-related amyloidosis (*57*, *58*). This is particularly relevant in the case of SAA because of its ability to form amyloid spontaneously at physiological temperatures, thereby suggesting that its interaction with ligands may have an effect on its in vivo amyloidogenicity (*30*).

Here we studied the effects of Cu^{2+}, Zn^{2+}, and Ca^{2+} on the structure and stability of hexameric SAA2.2. Our results showed that at physiological concentrations, Zn^{2+} stabilized SAA2.2, Cu^{2+} inhibited hexamer formation without destabilizing the monomer, and Ca^{2+} had a small destabilizing effect on all elements of SAA2.2 structure. As the concentration of Cu^{2+}, Zn^{2+}, and Ca^{2+} was increased, the effect on the stability of SAA2.2 was different for each metal but in all cases eventually resulted in SAA2.2 aggregation. Thus, this study identified Zn^{2+} as a potentially important SAA ligand, which along with the tremendous increase in SAA concentration may possibly serve to stabilize hexameric SAA during an acute phase response.

MATERIALS AND METHODS

Reagents and Sample Conditions. TPCK-treated trypsin and all chemicals, including $CuSO_4$, $ZnSO_4$, $CaCl_2$, glutaraldehyde, 2-amino-2-(hydroxymethyl)-1,3-propanediol (Tris), and 3-(*N*-morpholino)propanesulfonic acid (MOPS), were purchased from Sigma. Tris buffer (20 mM) was adjusted with HCl to pH 8.2, and MOPS buffer (20 mM) was adjusted with NaOH to pH 7.4. $CaCl_2$ was used instead of $CaSO_4$ because the lower solubility of the latter did not allow us to work with the more convenient high-concentration stock solutions of $CaSO_4$ used in the titration experiments.

SAA2.2 Expression and Purification. The murine SAA2.2 cDNA was cloned into a pET21-a(+) vector and transformed into *Escherichia coli* strain BL21(DE3)pLysS competent cells, as previously described (*59*). The expression and purification of SAA2.2 were carried out as we described in previous studies (*28*, *31*).

SAA2.2 Hexamer Dissociation Monitored by Glutaraldehyde Cross-Linking (GCL). SAA2.2 samples [15 μL of a 0.20 mg/mL solution in 20 mM MOPS buffer (pH 7.4)] with or without $CuSO_4$, $ZnSO_4$, or $CaCl_2$ were preincubated at 25 °C overnight. Then 0.7% (v/v) glutaraldehyde was added and incubated at 25 °C for 20 min to cross-link the SAA2.2 hexamer. The cross-linking reaction was quenched with 0.1 M Tris buffer (pH 8.0), and the samples were then analyzed by sodium dodecyl sulfate−polyacrylamide gel electrophoresis (SDS−PAGE).

SAA2.2 Denaturation Monitored by Fluorescence Spectroscopy. A Hitachi F-4500 fluorescence spectrophotometer was used to monitor the tertiary structure of SAA2.2 at different temperatures and at different metal concentrations. An excitation wavelength of 295 nm was used to exclusively excite the tryptophan residues, and the excitation slit width was set at 5 nm. The emission wavelength was measured from 300 to 400 nm using a slit width of 10 nm. SAA2.2 samples (27 μg/mL, in Tris buffer) containing different concentrations of $CuSO_4$, $ZnSO_4$, or $CaCl_2$ were prepared from the same stock solution. Each sample was incubated at the different temperatures for 15 min before the spectrum was recorded at a scan rate of 60 nm/min. Each experiment was repeated three times. The sample temperature was controlled with a water bath, and the exact temperature inside the cell was calculated from a temperature calibration curve obtained using a wire thermometer.

SAA2.2 Denaturation Monitored by Circular Dichroism (CD). The far-ultraviolet (UV) CD spectra of SAA2.2 samples (27 μg/mL, in Tris buffer) containing $CuSO_4$, $ZnSO_4$, or $CaCl_2$ were recorded on an OLIS CD instrument using a 2.0 mm pathway quartz cuvette. For thermal denaturation experiments, each temperature point was stabilized for 15 min before a wavelength scan was collected using a wavelength increment of 0.5 nm and a signal averaging of 2 s/point for 260−230 nm and 8 s/point for 230−200 nm. The sample temperature was controlled as described above for the fluorescence experiments. The experiment was repeated three times.

Limited Proteolysis by Trypsin. SAA2.2 samples (0.20 mg/mL, with or without metal ion) were partially digested with TPCK-treated trypsin at room temperature for 20 min and then immediately analyzed by SDS−PAGE. The SAA2.2:trypsin ratio was 120:1 (w/w).

RESULTS

Effect of Metals on the Quaternary Structure of SAA2.2. Hexameric SAA2.2 is marginally stable and dissociates to the monomer at mild temperatures with a transition midpoint

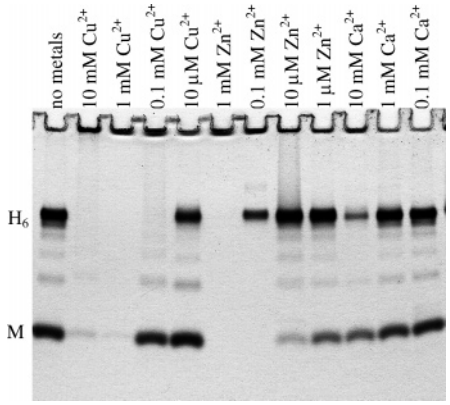

FIGURE 1: Effects of Cu^{2+}, Zn^{2+}, and Ca^{2+} on the quaternary structure of SAA2.2. SAA2.2 samples [0.20 mg/mL, in 20 mM MOPS (pH 7.4)] were incubated for 24 h with $CuSO_4$, $ZnSO_4$, or $CaCl_2$ and then crossed-linked for 20 min with 0.7% (v/v) glutaraldehyde. Samples were analyzed by SDS−PAGE. Notice that SAA2.2 forms aggregates in the presence of 1 mM Cu and Zn, and 10 mM Ca, and therefore does not enter the gel after cross-linking.

(T_m) of ~32 °C (*30*). Therefore, we first preincubated SAA2.2 samples overnight at 25 °C so that significant amounts of monomer would be in equilibrium with the hexamer and thus easily reveal the effect of Cu^{2+}, Zn^{2+}, or Ca^{2+} on the quaternary structure of SAA2.2. To monitor the quaternary structure of SAA2.2, we used glutaraldehyde cross-linking (GCL), a convenient method for trapping the oligomeric state of a protein for subsequent analysis by SDS−PAGE (*60*). We have used GCL very effectively in previous studies to trap the SAA2.2 hexamer under different sample conditions (*28*−*31*). Figure 1 (lane 1) shows that in the absence of metals there was a significant amount of SAA2.2 monomer present at 25 °C, but the top of the gel was clear, indicating that no high-molecular weight species were formed. In the presence of 10 μM Cu^{2+}, there was a slight decrease in the hexamer to monomer (H_6:M_1) ratio, suggesting that Cu^{2+} destabilized the hexamer. When incubated in 0.1 mM Cu^{2+}, the hexamer completely disappeared due mostly to its dissociation to the monomer, although some higher-molecular weight aggregates were also formed and trapped at the top of the well. The aggregation of SAA2.2 was exacerbated in 1 mM Cu^{2+}, resulting in nearly complete aggregation of the protein.

The effect of Zn^{2+} on the hexameric structure of SAA2.2 was the opposite of that of Cu^{2+} at 1−100 μM but similar to that at 1 mM (Figure 1). At 1 μM Zn^{2+}, there was a significant increase in the H_6:M_1 ratio, and at 10 μM Zn^{2+}, the hexamer was the predominant species, suggesting that Zn^{2+} stabilized the SAA2.2 hexamer. In 0.1 mM Zn^{2+}, the monomer was totally absent; however, the hexamer amount also decreased, and significant amounts of SAA2.2 aggregated and became trapped in the loading well. In the presence of 1 mM Zn^{2+}, SAA2.2 aggregated extensively, just like it did with 1 mM Cu^{2+}. Thus, Cu^{2+} destabilized hexameric SAA2.2 at concentrations below 100 μM, whereas Zn^{2+} stabilized the hexamer. Despite this opposite effect on the structure of SAA2.2, both 1 mM Cu^{2+} and 1 mM Zn^{2+} caused the total aggregation of SAA2.2.

In the case of Ca^{2+}, there was no effect on the quaternary structure of SAA2.2 at metal concentrations up to 0.1 mM (Figure 1). Even at 1 mM Ca^{2+}, there appeared to be only a slight increase in the H_6:M_1 ratio, but at 10 mM Ca^{2+}, there was a decrease in the H_6:M_1 ratio along with a decrease in the population of both species due to SAA2.2 aggregation. Thus, the GCL/SDS−PAGE results show that low micromolar concentrations of Cu^{2+} and Zn^{2+} destabilized and stabilized hexameric SAA2.2, respectively, whereas concentrations of ≥1 mM caused the complete aggregation of the protein. In contrast, the effect of Ca^{2+} on the hexameric structure of SAA2.2 was minimal even at low millimolar concentrations but caused some aggregation at 10 mM. To further investigate the effects of these metals on the structure and stability of SAA2.2, we monitored the temperature-induced denaturation of the protein using fluorescence and circular dichroism (CD) spectroscopy.

Effect of Metals on the Tertiary Structure of SAA2.2. Fluorescence spectroscopy was used to monitor the thermal denaturation of SAA2.2 in the presence of various concentrations of metals. The goal was to determine whether the metals were able to affect the stability of SAA2.2 in a manner consistent with and complementary to the results obtained by GCL/SDS−PAGE. We had to use a much lower SAA2.2 concentration and a shorter incubation time (27 μg/mL and 15 min, respectively) compared to those used in the GCL/SDS−PAGE experiments (0.20 mg/mL and 24 h, respectively) to avoid aggregation, which would otherwise occur as previously shown (*30*). We used an excitation wavelength of 295 nm to selectively excite the three Trp residues in SAA2.2 located at positions 17, 28, and 52, the first two of which are located in the hydrophobic N-terminus of SAA2.2. Because fluorescence intensity varies inversely with temperature, we monitored the change in the emission wavelength of maximum fluorescence (λ_{max}) to probe the denaturation of SAA2.2. The λ_{max} is a convenient way to monitor protein denaturation because it is sensitive to the environment of tryptophan and can change from ~320 to ~355 nm when a buried tryptophan is exposed to the solvent upon unfolding. We have previously shown that the λ_{max} of SAA2.2 changes from 340 to 352 nm upon denaturation, suggesting that the tryptophan residues in SAA2.2 are on average only partially buried (*29*, *30*).

The temperature denaturation of SAA2.2 was carried out in the presence of different concentrations of Cu^{2+}, Zn^{2+}, and Ca^{2+}, and some representative transitions are shown in Figure 2A−C. The transition midpoint temperature (T_m) was plotted versus metal concentration, and the resulting plots are shown in Figure 2D−F. The T_m values did not change significantly at Cu^{2+} and Ca^{2+} concentrations up to 100 μM and 1 mM, respectively, but then decreased as the concentration of metal increased. In contrast, at ~4 μM Zn^{2+}, there was a 4−5 °C increase in the T_m of SAA2.2 (Figure 2B,E) and an ~3 nm decrease in the λ_{max} (Figure 2B and data not shown), consistent with the stabilizing effect of Zn^{2+} observed in Figure 1. Oddly, a further increase in the concentration of Zn^{2+} led to a decrease in T_m (Figure 2E). We speculate that this may be caused by a combination of the fragile hexamer−monomer equilibrium and possible binding of Zn^{2+} to the monomer (like Cu^{2+}) when the concentration of Zn^{2+} exceeds a 2-fold molar excess. This equilibrium shift toward the monomer would be enhanced by the 7-fold lower SAA2.2 concentration used in the fluorescence compared to the GCL/SDS−PAGE experiments.

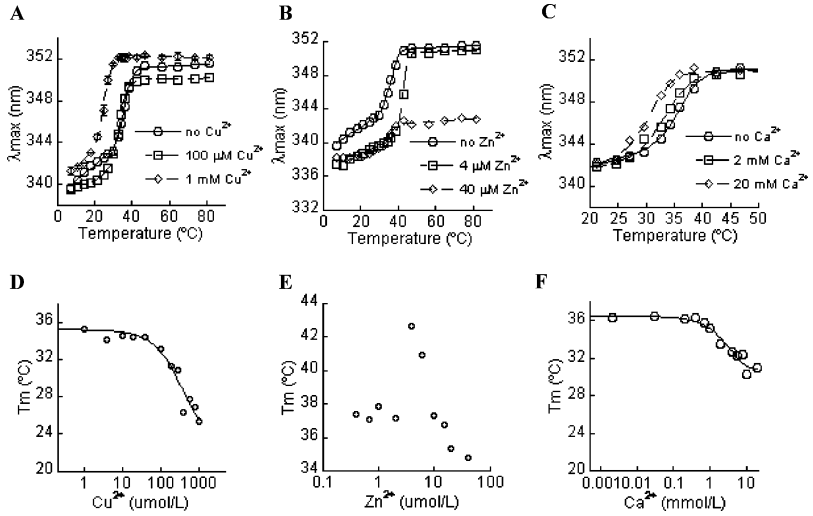

FIGURE 2: SAA2.2 thermal denaturation monitored by tryptophan fluorescence spectroscopy. (A−C) The emission λ_{max} was plotted against sample temperature, and the average values from three different experiments were shown. Standard deviation values were similar for all experiments, but for clarity, only the error bars corresponding to the SAA2.2 sample containing 1 mM Cu^{2+} are shown. (D−F) Transition midpoint temperature (T_m) plotted against metal ion concentration. Each sample contained 27 μg/mL (2.3 μM) SAA2.2 in Tris buffer. For a quantitative comparison of the metal cation effects, we assumed that the thermal denaturation of SAA2.2 involved a simple two-state transition, although no thermodynamic information could be obtained due to the irreversibility of the transitions.

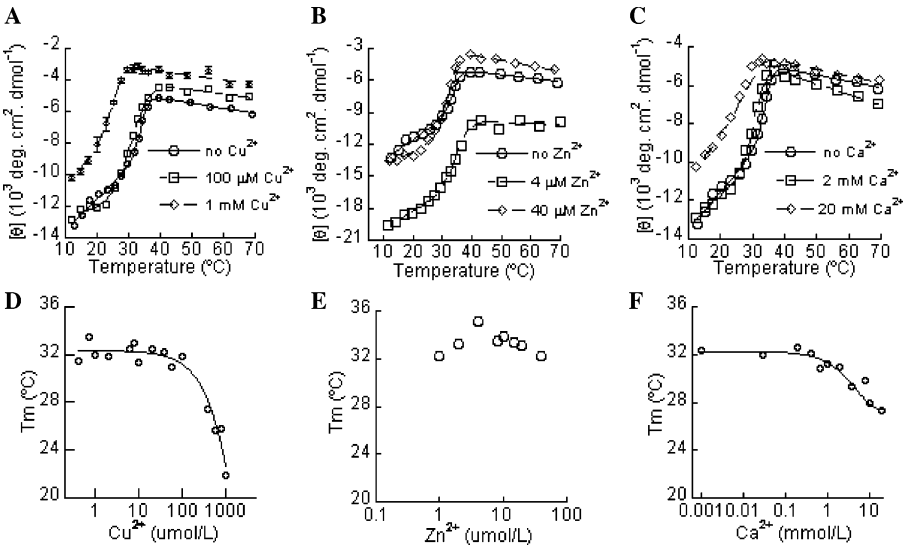

FIGURE 3: SAA2.2 thermal denaturation monitored by far-UV CD. (A−C) The molar residue ellipticity ($MRE_{222-255}$ or [θ]) was plotted against sample temperature, and the average values from three different experiments are shown. Standard deviation values were similar for all experiments, but for clarity, only the error bars corresponding to the SAA2.2 sample containing 1 mM Cu^{2+} are shown. (D−F) T_m was plotted against the metal ion concentration. Each sample contained 27 μg/mL (2.3 μM) SAA2.2 and Tris buffer. For a quantitative comparison of the metal cation effects, we assumed that the thermal denaturation of SAA2.2 involved a simple two-state transition, although no thermodynamic information could be obtained due to the irreversibility of the transitions. The smooth curves from Figure 2D−F were included to provide visual guidance.

Effect of Metals on the Secondary Structure of SAA2.2. Far-UV CD spectroscopy was used to measure the changes in secondary structure upon thermal denaturation of SAA2.2 in the presence of Cu^{2+}, Zn^{2+}, or Ca^{2+}. The molar residue ellipticity (MRE) values at 222 nm were plotted versus temperature to yield denaturation transitions like the representative ones shown in Figure 3A−C. The T_m was plotted against the concentration of metals to determine their effect on the stability of the secondary structure of SAA2.2 (Figure 3D−F). The CD and fluorescence data are in excellent agreement, although the T_m values from the latter were a few degrees higher. The steeper slopes in the pretransition stages from CD experiments (Figure 3A−C) may be responsible for causing an apparent decrease in T_m values compared to the fluorescence data (Figure 2A−C). Interestingly, like the decrease in λ_{max} seen for SAA2.2 upon addition of Zn^{2+}, the MRE values within the pretransition became more negative in the presence of Zn^{2+} (Figure 4), altogether suggesting that Zn^{2+} binds to and shifts the equilibrium of SAA2.2 toward the hexamer, causing an increase in the degree of burial of tryptophan residues and an increase in helical structure content.

Limited Trypsin Proteolysis. Limited proteolysis is a simple method for obtaining general information about protein stability and for identifying regions within a protein that may be more exposed to the solvent. We used limited trypsin digestion to gain more insight about the effect of Cu^{2+}, Zn^{2+}, and Ca^{2+} on the structure of SAA2.2 (Figure 5). SAA2.2 has 14 Lys or Arg residues at positions 18, 24, 29, 33, 38, 46, 56, 61, 70, 83, 86, 89, 95, and 102,

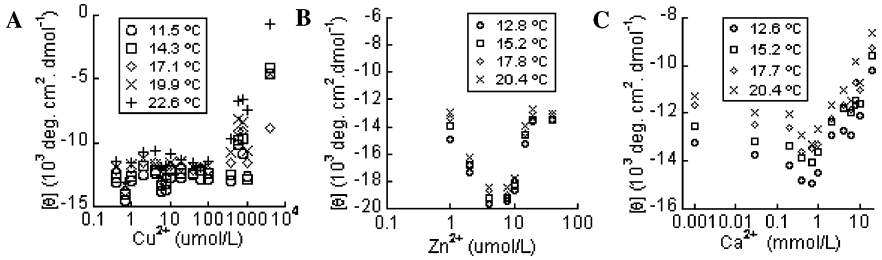

FIGURE 4: Effect of metals on the far-UV CD signal of native SAA2.2. The molar residue ellipticity [θ] of the pretransition baseline was plotted against the metal ion concentration. Data were obtained from the experiments described in the legend of Figure 3.

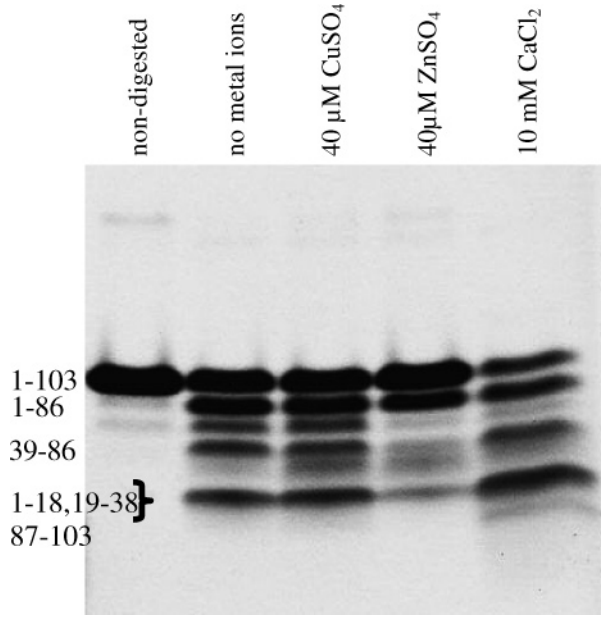

FIGURE 5: Limited trypsin proteolysis of SAA2.2 analyzed by SDS−PAGE. The SAA2.2 concentration in all samples was 17 μM. Trypsin was incubated with SAA2.2 at room temperature for 20 min, using a SAA2.2:trypsin ratio of 120:1 (w/w). The identification of the fragments was based on HPLC/mass spectrometry analysis carried out in previous studies (*28*−*30*).

and we have previously shown by limited trypsin proteolysis that Arg86 is the residue most vulnerable to trypsin cleavage followed by residue 38 (*28*). On the basis of the GCL/SDS−PAGE data (Figure 1), in the presence of 40 μM Cu^{2+} or Zn^{2+}, SAA2.2 (17 μM) should largely exist as a monomer or hexamer, respectively; in the case of 10 mM Ca^{2+}, SAA2.2 would be expected to exist in a mixture of hexamer, monomer, and aggregates. Figure 5 shows that the limited trypsin proteolysis of SAA2.2 in the presence of 40 μM Cu^{2+} is similar to that of SAA2.2 without metals. This result is consistent with our published data showing very similar proteolytic profiles for hexameric and monomeric SAA2.2 under mild denaturing conditions (*29*). It is also consistent with the fluorescence (Figure 2) and CD (Figure 3) data, which showed that 40 μM Cu^{2+} had no effect on the stability of the tertiary and secondary structure of SAA2.2. In the presence of Zn^{2+}, although the proteolysis pattern was the same, SAA2.2 was more resistant to trypsin proteolysis, consistent with the greater stability of SAA2.2 (Figures 1−3). In 10 mM Ca^{2+}, SAA2.2 was more susceptible to trypsin proteolysis, a result that agrees with the significant decrease in the quaternary, tertiary, and secondary structure stability of SAA2.2 under these conditions (Figures 1−3).

DISCUSSION

The Structure and Stability of SAA2.2 Are Susceptible to Cu^{2+}, Zn^{2+}, and Ca^{2+}. The marginal stability of SAA2.2 suggests that its structure, stability, and function may be modulated in vivo through ligand binding. Here we have shown that the metals Cu^{2+}, Zn^{2+}, and Ca^{2+} have different effects on SAA2.2 (summarized in Table 1). The decreased population of hexameric SAA2.2 in the presence of 10−100 μM Cu^{2+} without a significant effect on the tertiary and secondary structure, along with the unchanged profile of limited trypsin proteolysis, suggests that Cu^{2+} binds weakly to SAA2.2 at a site that blocks hexamer formation while preserving the structure and stability of the monomer. From the SAA2.2 H_6:M_1 ratio in GCL experiments (Figure 1), the binding affinity of Cu^{2+} for the SAA2.2 monomer seems to be around tens of micromolar. In quite the opposite manner, Zn^{2+} binds to SAA2.2 with higher affinity and in a way that stabilizes the quaternary, tertiary, and secondary structures of the protein. It is not clear at this point why the stabilizing effect of Zn^{2+} on the tertiary and secondary structure of SAA2.2 seems to peak at ~4 μM (see Figures 2 and 3), but we suspect it may be related to the 7-fold lower SAA2.2 concentration (2.3 μM) used in these experiments. For example, 10 μM Zn^{2+} was not even equimolar to SAA2.2 (17 μM) in the GCL/SDS−PAGE and trypsin experiments but was equivalent to a 4-fold molar excess in the fluorescence and CD experiments. Perhaps the surplus of Zn^{2+} allowed it to bind to another lower-affinity region within SAA2.2, resulting in destabilization of the protein. Finally, the milder effects of Ca^{2+} demonstrate that this metal is not destabilizing to SAA2.2 until concentrations above 1 mM.

It would be interesting to know where the metals are binding within SAA2.2. Ca^{2+} may be binding to the proposed calcium binding motif (GPGG, residues 47−50), a highly conserved and solvent-exposed region of SAA (*43*). Since the three-dimensional structure of SAA2.2 is unknown, it is difficult to predict where Cu^{2+} and Zn^{2+} may be binding. Histidine is the most common ligand of Cu^{2+} and Zn^{2+} in proteins, and SAA2.2 has four His residues at positions 7, 36, 72, and 84. His7 is located on the polar side of the amphipathic N-terminal α-helical region of SAA2.2. His36 and His84 are near Arg38 and Arg86, respectively, the two sites most susceptible to trypsin cleavage. His72 is located in a polar region (GRGHEDT) that is predicted to be in a loop/disordered conformation. Thus, it seems that all four His residues in SAA2.2 are in solvent-exposed regions where they may interact with Cu^{2+} and Zn^{2+}. It is noteworthy that of these four histidine residues, only His36 and His72 are conserved in human SAA, whereas His7 and His84 are not

Table 1: Summary of the Effects of Metals on the Structure and Stability of SAA2.2

metal	effects
Cu^{2+}	10−100 μM Cu^{2+} shifts the hexamer−monomer equilibrium toward the latter without significantly affecting the stability of the tertiary and secondary structure; level of SAA2.2 aggregation increases at >100 μM Cu^{2+}
Zn^{2+}	1−10 μM Zn^{2+} stabilizes the SAA2.2 hexamer, with tertiary and secondary structure being optimally stabilized with an ~2-fold molar excess of Zn^{2+} (e.g., 4 μM); fluorescence λ_{max} decreases and CD signal becomes more negative; level of SAA2.2 aggregation increases at >100 μM Zn^{2+}
Ca^{2+}	has a negligible effect on SAA2.2 at ≤1 mM Ca^{2+} but is destabilizing between 1 and 10 mM; level of SAA2.2 aggregation increases at >10 mM Ca^{2+}

conserved residues in SAA from different species. Thus, if Zn^{2+} binding were to play a general role in SAA function, His36 and His72 would be two of the possible ligands.

The opposite effects of Cu^{2+} and Zn^{2+} on the structure and stability of SAA2.2 suggest that they bind to different regions. It is possible that the Cu^{2+} binding site may involve residues from the same subunit located in a loop region, thus blocking hexamer formation by directly interfering with monomer−monomer interactions. In contrast, Zn^{2+} binding may include one or more residues involved in the secondary and tertiary structure of SAA2.2, resulting in an increased stability of the monomer, and consequently of the hexamer as well. Alternatively, Zn^{2+} binding may involve residues from different subunits within the hexamer. In one scenario, His7 may serve as an intermolecular ligand of Zn^{2+} because in previous studies we had proposed that SAA2.2 may hexamerize by forming an α-helical bundle involving the amphipathic N-terminal region of each subunit (*31*). In the proposed hexamer, the lumen of the central pore would be largely hydrophilic with His7, Glu8, Asp15, and Asp22 facing the lumen and readily accessible to Zn^{2+} binding. Also, the decrease in the level of proteolytic cleavage at position 38 when SAA2.2 was incubated with Zn^{2+} also suggests that His36, which is nearly 100% conserved across different species, may serve as one of the Zn^{2+} ligands. Future mutational studies of the His residues in SAA2.2 should make it possible to probe the role of each residue in the binding of Cu^{2+} and Zn^{2+} to SAA2.2.

Biological Implications of the Effect of Metal Binding on SAA2.2. Because of the many biological functions and pathological conditions that have been linked to SAA, understanding their structural basis is intriguing, especially when considering its small size. The unknown three-dimensional structure of SAA, the dramatic increase in its concentration during inflammation, and the high level of conservation of SAA in all vertebrates enhance the mystery surrounding this protein. The discovery that SAA2.2 forms a hexamer that denatures to the monomer at 37 °C and spontaneously misfolds and aggregates into amyloid fibrils suggests that in vivo the structure and function of SAA are probably modulated by its concentration levels and by binding to ligands besides HDL. Indeed, it has been shown that during the acute phase response, not all SAA is bound to HDL (*61*). Thus, the effect of physiological concentrations of metals that we have reported here may have implications for SAA biology. For example, the increase in SAA concentration in conjunction with its binding to Zn^{2+} may serve to stabilize the hexamer, which we have shown to be unstable at 37 °C and totally dissociated at the feverlike temperature of 41 °C (*31*). Since SAA leaves the serum and accumulates at inflamed tissues and organs, this may partly explain why the concentration of Zn^{2+} in plasma decreases during the acute phase response from ~16 μM (*62*, *63*) to ~10 μM (*33*, *64*).

It remains to be determined whether binding of SAA to Ca^{2+} or Cu^{2+} has any biological relevance. The normal Ca^{2+} and Cu^{2+} concentrations in serum are ~2.5 mM (*65*, *66*) and ~20 μM (*62*, *63*), respectively, a concentration at which Ca^{2+} begins to destabilize SAA2.2 and Cu^{2+} blocks SAA hexamer formation. Thus, it is conceivable that binding of SAA to various metals and ligands might alter the balance among various SAA conformers, such as HDL-free hexamer, HDL-free monomer, HDL-bound monomer, and other oligomeric species (*31*). These different SAA structural forms may have different functions in vivo, and therefore, the different affinity of ligands for marginally stable SAA may play a role in modulating its structure and function during normal and inflammatory conditions.

Metal Binding May Affect the in Vivo Amyloidogenicity of SAA. Numerous studies have demonstrated that metal cations such as Zn^{2+} and Cu^{2+} can bind to amyloidogenic proteins and peptides and facilitate their aggregation (*52*, *67*). In our study, higher concentrations of Zn^{2+}, Ca^{2+}, and Cu^{2+} all induced the aggregation of SAA2.2, although the required minimum metal ion concentrations are different (Figure 1). The effect of Ca^{2+} is particularly relevant because it was found to induce the aggregation of SAA2.2 at physiological Ca^{2+} concentrations. In vivo, a slight increase in plasma Ca^{2+} concentration might destabilize SAA and facilitate amyloid formation, which would be consistent with the finding that AA amyloid deposits in vivo are rich in Ca^{2+} (*44*), the finding that physiological concentrations of calcium can accelerate the aggregation of the also marginally stable amyloid β-peptide (*53*), and our findings that Ca^{2+} stabilizes SAA amyloid fibrils in vitro (unpublished results). It will be interesting in future studies to probe the mechanism by which the various metals induce the aggregation of SAA and to characterize these aggregates in terms of morphology and stability. Furthermore, comparison between SAA isoforms with different in vivo amyloidogenicity may begin to reveal the molecular and structural basis for their different amyloidogenicity.

REFERENCES

1. Malle, E., and de Beer, F. C. (1996) Human serum amyloid A (SAA) protein: A prominent acute phase reactant for clinical practice, *Eur. J. Clin. Invest. 26*, 427−435.
2. Uhlar, C. M., and Whitehead, A. S. (1999) Serum amyloid A, the major vertebrate acute-phase reactant, *Eur. J. Biochem. 265*, 501−523.
3. Uhlar, C. M., Burgess, C. J., Sharp, P. M., and Whitehead, A. S. (1994) Evolution of the serum amyloid A (SAA) protein superfamily, *Genomics 19*, 228−235.
4. McAdam, K. P. W. J., and Sipe, J. D. (1976) Murine model for human secondary amyloidosis: Genetic variability of the acute-

phase serum protein SAA response to endotoxins and casein, *J. Exp. Med. 144*, 1121−1127.
5. De Beer, F. C., Mallya, R. K., Fagan, E. A., Lanham, J. G., Hughes, G. R., and Pepys, M. B. (1982) Serum amyloid-A protein concentration in inflammatory diseases and its relationship to the incidence of reactive systemic amyloidosis, *Lancet 2*, 213−234.
6. Meek, R. L., Urieli-Shoval, S., and Benditt, E. P. (1994) Expression of apolipoprotein serum amyloid A mRNA in human atherosclerotic lesions and cultured vascular cells: Implications for serum amyloid A function, *Proc. Natl. Acad. Sci. U.S.A. 91*, 3186−3190.
7. Urieli-Shoval, S., Meek, R. L., Hanson, R. H., Eriksen, N., and Benditt, E. P. (1994) Human serum amyloid A genes are expressed in monocyte/macrophage cell lines, *Am. J. Pathol. 145*, 650−660.
8. Urieli-Shoval, S., Cohen, P., Eisenberg, S., and Matzner, Y. (1998) Widespread expression of serum amyloid A in histologically normal human tissues. Predominant localization to the epithelium, *J. Histochem. Cytochem. 46*, 1377−1384.
9. O'Hara, R., Murphy, E. P., Whitehead, A. S., FitzGerald, O., and Bresnihan, B. (2000) Acute-phase serum amyloid A production by rheumatoid arthritis synovial tissue, *Arthritis Res. 2*, 142−144.
10. Kumon, Y., Suehiro, T., Hashimoto, K., Nakatani, K., and Sipe, J. D. (1999) Local expression of acute phase serum amyloid A mRNA in rheumatoid arthritis synovial tissue and cells, *J. Rheumatol. 26*, 785−790.
11. Thorn, C. F., Lu, Z. Y., and Whitehead, A. S. (2003) Tissue-specific regulation of the human acute-phase serum amyloid A genes, SAA1 and SAA2, by glucocorticoids in hepatic and epithelial cells, *Eur. J. Immunol. 33*, 2630−2639.
12. Tanaka, F., Migita, K., Kawabe, Y., Aoyagi, T., Ida, H., Kawakami, A., and Eguchi, K. (2004) Interleukin-18 induces serum amyloid A (SAA) protein production from rheumatoid synovial fibroblasts, *Life Sci. 74*, 1671−1679.
13. Upragarin, N., Landman, W. J., Gaastra, W., and Gruys, E. (2005) Extrahepatic production of acute phase serum amyloid A, *Histol. Histopathol. 20*, 1295−1307.
14. Gonzalez, S. F., Buchmann, K., and Nielsen, M. E. (2006) *Ichthyophthirius multifiliis* infection induces massive up-regulation of serum amyloid A in carp (*Cyprinus carpio*), *Vet. Immunol. Immunopathol. 115*, 172−178.
15. Libby, P., Ridker, P. M., and Maseri, A. (2002) Inflammation and atherosclerosis, *Circulation 105*, 1135−1143.
16. Marx, J. (2004) Inflammation and cancer: The link grows stronger, *Science 306*, 966−968.
17. Tuppo, E. E., and Arias, H. R. (2005) The role of inflammation in Alzheimer's disease, *Int. J. Biochem. Cell Biol. 37*, 289−305.
18. Aggarwal, B. B., Shishodia, S., Sandur, S. K., Pandey, M. K., and Sethi, G. (2006) Inflammation and cancer: How hot is the link? *Biochem. Pharmacol. 72*, 1605−1621.
19. Biran, H., Friedman, N., Neumann, L., Pras, M., and Shainkin-Kestenbaum, R. (1986) Serum amyloid A (SAA) variations in patients with cancer: Correlation with disease activity, stage, primary site, and prognosis, *J. Clin. Pathol. 39*, 794−797.
20. Kindy, M. S., Yu, J., Guo, J. T., and Zhu, H. (1999) Apolipoprotein Serum Amyloid A in Alzheimer's Disease, *J. Alzheimer's Dis. 1*, 155−167.
21. Urieli-Shoval, S., Linke, R. P., and Matzner, Y. (2000) Expression and function of serum amyloid A, a major acute-phase protein, in normal and disease states, *Curr. Opin. Hematol. 7*, 64−69.
22. Chung, T. F., Sipe, J. D., McKee, A., Fine, R. E., Schreiber, B. M., Liang, J. S., and Johnson, R. J. (2000) Serum amyloid A in Alzheimer's disease brain is predominantly localized to myelin sheaths and axonal membrane, *Amyloid 7*, 105−110.
23. Cunnane, G. (2001) Amyloid proteins in pathogenesis of AA amyloidosis, *Lancet 358*, 4−5.
24. Gillmore, J. D., Lovat, L. B., Persey, M. R., Pepys, M. B., and Hawkins, P. N. (2001) Amyloid load and clinical outcome in AA amyloidosis in relation to circulating concentration of serum amyloid A protein, *Lancet 358*, 24−29.
25. Levin, M., Franklin, E. C., Frangione, B., and Pras, M. (1972) The amino acid sequence of a major nonimmunoglobulin component of some amyloid fibrils, *J. Clin. Invest. 51*, 2773−2776.
26. Husebekk, A., Skogen, B., Husby, G., and Marhaug, G. (1985) Transformation of amyloid precursor SAA to protein AA and incorporation in amyloid fibrils in vivo, *Scand. J. Immunol. 21*, 283−287.
27. Ericsson, L. H., Eriksen, N., Walsh, K. A., and Benditt, E. P. (1987) Primary structure of duck amyloid protein A. The form deposited in tissues may be identical to its serum precursor, *FEBS Lett. 218*, 11−16.
28. Wang, L., Lashuel, H. A., Walz, T., and Colón, W. (2002) Murine apolipoprotein serum amyloid A in solution forms a hexamer containing a central channel, *Proc. Natl. Acad. Sci. U.S.A. 99*, 15947−15952.
29. Wang, L., and Colon, W. (2005) Urea-induced denaturation of apolipoprotein serum amyloid A reveals marginal stability of hexamer, *Protein Sci. 14*, 1811−1817.
30. Wang, L., Lashuel, H. A., and Colon, W. (2005) From hexamer to amyloid: Marginal stability of apolipoprotein SAA2.2 leads to in vitro fibril formation at physiological temperature, *Amyloid 12*, 139−148.
31. Wang, L., and Colón, W. (2004) The interaction between apolipoprotein serum amyloid A and high-density lipoprotein, *Biochem. Biophys. Res. Commun. 317*, 157−161.
32. Sobocinski, P. Z., Canterbury, W. J., Jr., Hauer, E. C., and Beall, F. A. (1979) Induction of hypozincemia and hepatic metallothionein synthesis in hypersensitivity reactions, *Proc. Soc. Exp. Biol. Med. 160*, 175−179.
33. Kushner, I. (1982) The phenomenon of the acute phase response, *Ann. N.Y. Acad. Sci. 389*, 39−48.
34. Fraker, P. J., King, L. E., Laakko, T., and Vollmer, T. L. (2000) The dynamic link between the integrity of the immune system and zinc status, *J. Nutr. 130*, 1399S-1406S.
35. Rink, L., and Gabriel, P. (2000) Zinc and the immune system, *Proc. Nutr. Soc. 59*, 541−552.
36. Dardenne, M. (2002) Zinc and immune function, *Eur. J. Clin. Nutr. 56* (Suppl. 3), S20−S23.
37. Ibs, K. H., and Rink, L. (2003) Zinc-altered immune function, *J. Nutr. 133*, 1452S−1456S.
38. Conforti, A., Franco, L., Milanino, R., Totorizzo, A., and Velo, G. P. (1983) Copper metabolism during acute inflammation: Studies on liver and serum copper concentrations in normal and inflamed rats, *Br. J. Pharmacol. 79*, 45−52.
39. Oliva, J. C., Castell, M., Queralt, J., and Castellote, C. (1987) Effect of chronic inflammation on copper and zinc metabolism, *Rev. Esp. Fisiol. 43*, 25−31.
40. Lei, K. Y. (1991) Dietary copper: Cholesterol and lipoprotein metabolism, *Annu. Rev. Nutr. 11*, 265−283.
41. Kisilevsky, R., and Subrahmanyan, L. (1992) Serum amyloid A changes high density lipoprotein's cellular affinity. A clue to serum amyloid A's principal function, *Lab. Invest. 66*, 778−785.
42. Liang, J. S., Schreiber, B. M., Salmona, M., Phillip, G., Gonnerman, W. A., de Beer, F. C., and Sipe, J. D. (1996) Amino terminal region of acute phase, but not constitutive, serum amyloid A (apoSAA) specifically binds and transports cholesterol into aortic smooth muscle and HepG2 cells, *J. Lipid Res. 37*, 2109−2116.
43. Turnell, W., Sarra, R., Glover, I. D., Baum, J. O., Caspi, D., Baltz, M. L., and Pepys, M. B. (1986) Secondary structure prediction of human SAA1. Presumptive identification of calcium and lipid binding sites, *Mol. Biol. Med. 3*, 387−407.
44. Kula, R. W., Engel, W. K., and Line, B. R. (1977) Scanning for soft-tissue amyloid, *Lancet 1*, 92−93.
45. Danielsen, B., Sorensen, I. J., Nybo, M., Nielsen, E. H., Kaplan, B., and Svehag, S. E. (1997) Calcium-dependent and -independent binding of the pentraxin serum amyloid P component to glycosaminoglycans and amyloid proteins: Enhanced binding at slightly acid pH, *Biochim. Biophys. Acta 1339*, 73−78.
46. Jobling, M. F., Huang, X., Stewart, L. R., Barnham, K. J., Curtain, C., Volitakis, I., Perugini, M., White, A. R., Cherny, R. A., Masters, C. L., Barrow, C. J., Collins, S. J., Bush, A. I., and Cappai, R. (2001) Copper and zinc binding modulates the aggregation and neurotoxic properties of the prion peptide PrP106−126, *Biochemistry 40*, 8073−8084.
47. Millhauser, G. L. (2004) Copper binding in the prion protein, *Acc. Chem. Res. 37*, 79−85.
48. Atwood, C. S., Moir, R. D., Huang, X., Scarpa, R. C., Bacarra, N. M., Romano, D. M., Hartshorn, M. A., Tanzi, R. E., and Bush, A. I. (1998) Dramatic aggregation of Alzheimer Aβ by Cu(II) is induced by conditions representing physiological acidosis, *J. Biol. Chem. 273*, 12817−12826.
49. Liu, S. T., Howlett, G., and Barrow, C. J. (1999) Histidine-13 is a crucial residue in the zinc ion-induced aggregation of the Aβ peptide of Alzheimer's disease, *Biochemistry 38*, 9373−9378.
50. House, E., Collingwood, J., Khan, A., Korchazkina, O., Berthon, G., and Exley, C. (2004) Aluminium, iron, zinc and copper influence the in vitro formation of amyloid fibrils of Aβ42 in a

manner which may have consequences for metal chelation therapy in Alzheimer's disease, *J. Alzheimer's Dis. 6*, 291−301.
51. Cuajungco, M. P., Frederickson, C. J., and Bush, A. I. (2005) Amyloid-β metal interaction and metal chelation, *Subcell. Biochem. 38*, 235−254.
52. Khan, A., Ashcroft, A. E., Higenell, V., Korchazhkina, O. V., and Exley, C. (2005) Metals accelerate the formation and direct the structure of amyloid fibrils of NAC, *J. Inorg. Biochem. 99*, 1920−1927.
53. Isaacs, A. M., Senn, D. B., Yuan, M., Shine, J. P., and Yankner, B. A. (2006) Acceleration of amyloid β-peptide aggregation by physiological concentrations of calcium, *J. Biol. Chem. 281*, 27916−27923.
54. Paik, S. R., Shin, H. J., Lee, J. H., Chang, C. S., and Kim, J. (1999) Copper(II)-induced self-oligomerization of α-synuclein, *Biochem. J. 340* (Part 3), 821−828.
55. Uversky, V. N., Li, J., and Fink, A. L. (2001) Metal-triggered structural transformations, aggregation, and fibrillation of human α-synuclein. A possible molecular NK between Parkinson's disease and heavy metal exposure, *J. Biol. Chem. 276*, 44284−44296.
56. Lowe, R., Pountney, D. L., Jensen, P. H., Gai, W. P., and Voelcker, N. H. (2004) Calcium(II) selectively induces α-synuclein annular oligomers via interaction with the C-terminal domain, *Protein Sci. 13*, 3245−3252.
57. Eakin, C. M., Knight, J. D., Morgan, C. J., Gelfand, M. A., and Miranker, A. D. (2002) Formation of a copper specific binding site in non-native states of β-2-microglobulin, *Biochemistry 41*, 10646−10656.
58. Eakin, C. M., and Miranker, A. D. (2005) From chance to frequent encounters: Origins of β2-microglobulin fibrillogenesis, *Biochim. Biophys. Acta 1753*, 92−99.
59. Liang, J., Elliott-Bryant, R., Hajri, T., Sipe, J. D., and Cathcart, E. S. (1998) A unique amyloidogenic apolipoprotein serum amyloid A (apoSAA) isoform expressed by the amyloid resistant CE/J mouse strain exhibits higher affinity for macrophages than apoSAA1 and apoSAA2 expressed by amyloid susceptible CBA/J mice, *Biochim. Biophys. Acta 1394*, 121−126.
60. Craig, W. S. (1988) Determination of quaternary structure of an active enzyme using chemical cross-linking with glutaraldehyde, *Methods Enzymol. 156*, 333−345.
61. Hajri, T., Elliott-Bryant, R., Sipe, J. D., Liang, J. S., Hayes, K. C., and Cathcart, E. S. (1998) The acute phase response in apolipoprotein A-1 knockout mice: Apolipoprotein serum amyloid A and lipid distribution in plasma high density lipoproteins, *Biochim. Biophys. Acta 1394*, 209−218.
62. Aruoma, O. I., Reilly, T., MacLaren, D., and Halliwell, B. (1988) Iron, copper and zinc concentrations in human sweat and plasma: The effect of exercise, *Clin. Chim. Acta 177*, 81−87.
63. Rukgauer, M., Klein, J., and Kruse-Jarres, J. D. (1997) Reference values for the trace elements copper, manganese, selenium, and zinc in the serum/plasma of children, adolescents, and adults, *J. Trace Elem. Med. Biol. 11*, 92−98.
64. Brown, K. H. (1998) Effect of infections on plasma zinc concentration and implications for zinc status assessment in low-income countries, *Am. J. Clin. Nutr. 68*, 425S−429S.
65. Lester, E., and Varghese, Z. (1977) Differences in the calcium concentration of serum and plasma initially and after storage, *Ann. Clin. Biochem. 14*, 39−44.
66. Boetefur, A. K., and Muller-Plathe, O. (1995) Evaluation of a new method for determining the total calcium concentration using diluted plasma and an ion-selective electrode, *Eur. J. Clin. Chem. Clin. Biochem. 33*, 749−754.
67. Agrimi, U., and Di Guardo, G. (1993) Amyloid, amyloid-inducers, cytokines and heavy metals in scrapie and other human and animal subacute spongiform encephalopathies: Some hypotheses, *Med. Hypotheses 40*, 113−116.

BI602629Y